

The photometric period in ES Ceti

C. M. Copperwheat,^{1*} T. R. Marsh,¹ V. S. Dhillon,² S. P. Littlefair,² P. A. Woudt,³
B. Warner,³ J. Patterson,⁴ D. Steeghs,¹ J. Kemp,⁴ E. Armstrong⁴ and R. Rea⁵

¹*Department of Physics, University of Warwick, Coventry CV4 7AL*

²*Department of Physics and Astronomy, University of Sheffield, Sheffield S3 7RH*

³*Astrophysics, Cosmology and Gravity Centre, Department of Astronomy, University of Cape Town, Private Bag X3, Rondebosch 7701, South Africa*

⁴*Department of Astronomy, Columbia University, 550 West 120th Street, New York, NY10027, USA*

⁵*CBA (Nelson), 8 Regent Lane, Richmond, Nelson, New Zealand*

Accepted 2011 January 18. Received 2011 January 10; in original form 2010 November 2

ABSTRACT

We present ULTRACAM photometry of ES Cet, an ultracompact binary with a 620-s orbital period. The mass transfer in systems such as this one is thought to be driven by gravitational radiation, which causes the binary to evolve to longer periods since the semidegenerate donor star expands in size as it loses mass. We supplement these ULTRACAM+William Herschel Telescope (WHT) data with observations made with smaller telescopes around the world over a 9-yr baseline. All of the observations show variation on the orbital period, and by timing this variation we track the period evolution of this system. We do not detect any significant departure from a linear ephemeris, implying a donor star that is of small mass and close to a fully degenerate state. This finding favours the double white dwarf formation channel for this AM Canum Venaticorum (AM CVn) star. An alternative explanation is that the system is in the relatively short-lived phase in which the mass transfer rate climbs towards its long-term value.

Key words: binaries: close – stars: individual: ES Ceti – novae, cataclysmic variables – white dwarfs.

1 INTRODUCTION

Ultracompact binaries with periods of the order of tens of minutes or less have attracted much attention in recent years. These systems consist of a primary white dwarf with a companion star that is also at least partially degenerate. Close double-degenerate binaries are one of the proposed progenitor populations of Type Ia supernovae (Kotak 2008; Di Stefano 2010; Gilfanov & Bogdán 2010), as well as the recently proposed subluminous ‘Ia’ supernovae (Bildsten et al. 2007; Kasliwal et al. 2010). They are of interest from a binary formation and evolution point of view, with the short periods implying at least one common envelope phase in the history of the binary, and the chemical composition suggesting helium white dwarfs, helium stars or cataclysmic variables (CVs) with evolved secondaries as possible progenitors (Nelemans et al. 2001, 2010). The mass transfer in these systems is thought to be driven by angular momentum loss as a result of gravitational radiation. These sources are predicted to be among the strongest gravitational wave sources in the sky (Nelemans, Yungelson & Portegies Zwart 2004) and are the only class of binary with examples already known which will be detectable by the gravitational wave observatory *LISA* (Stroerer & Vecchio 2006; Roelofs, Nelemans & Groot 2007b).

The two systems with the shortest known periods are HM Cnc (324 s, Roelofs et al. 2010) and V407 Vul (569 s, Haberl & Motch 1995). The exact nature of these systems is unclear: the two leading models are the unipolar induction (UI) model (Wu et al. 2002) and the direct-impact accretion model (Marsh & Steeghs 2002; Roelofs et al. 2010). There are also 23 known systems with longer periods ranging from 620 to 3906 s [the AM Canum Venaticorum (AM CVn) stars; see Solheim 2010 for a recent review]. The natures of these systems are better established: the spectra show an absence of hydrogen and the presence of helium lines, many of which are the double-peaked emission lines characteristic of sources accreting via a disc (Marsh 1999; Morales-Rueda et al. 2003). These systems are clearly accreting and are the helium equivalent of the CV stars.

Gravitational radiation has a huge influence on these systems, driving the evolution and determining the orbital period distribution, luminosities and numbers. Measurements of the time derivative of the orbital period P for V407 Vul and HM Cnc have shown the periods in these systems to be decreasing (Hakala et al. 2003; Hakala, Ramsay & Byckling 2004; Ramsay et al. 2005; Strohmayer 2005). This is consistent with the UI model and contrary to what might be expected for accretion. In an accreting double-degenerate system, the gravitational radiation should drive the binary towards longer orbital periods. However, if the mass transfer in an accreting double-degenerate system is significantly lower than its equilibrium value, due to either some non-secular process (Marsh & Nelemans

*E-mail: c.copperwheat@warwick.ac.uk

2005) or the binary being in its mass transfer turn-on phase (Willems & Kalogera 2005; D'Antona et al. 2006; Deloye & Taam 2006), then a decreasing binary period is possible. The counter argument to this is that such phases are expected to be short although Deloye & Taam (2006) calculated that the early contact phase can last much longer (10^3 – 10^6 yr) than originally thought.

To date, no period derivative has been measured in any of the longer period AM CVn stars. Since these are unambiguously accreting binaries, we would expect to detect an increasing period in these objects. Additionally, it is not certain that gravitational radiation is the dominant angular momentum loss mechanism for the ultracompact binary stars: some other mechanism, such as the magnetic braking observed in CVs, could be operating to drive the evolution at a higher rate than assumed in current models (Farmer & Roelofs 2010). These astrophysical issues will in the future be important for the use of these systems for the verification of *LISA* as they can make the difference between detectability or non-detectability (Stroerer & Vecchio 2006).

In order to address this issue, we have conducted a long-term timing study of the AM CVn star ES Ceti (Warner & Woudt 2002). This system shows a 620-s optical modulation which is complex in structure and varies on a night-by-night basis (Espaillat et al. 2005). Spectroscopic observations have confirmed that this is the orbital period, and also show the double-peaked helium emission lines which imply the presence of an accretion disc in this system (Steehgs, in preparation). ES Ceti is the ideal subject for a timing study, since it is the shortest period ultracompact binary population after V407 Vul and HM Cnc. It potentially connects these two systems to the rest of the AM CVn population: the period of ES Ceti is only 51 s greater than V407 Vul, so ES Ceti may also be in the mass transfer turn-on phase. If, however, ES Ceti has already evolved on to the long-term and stable AM CVn path of lengthening period, then we would expect the period evolution to be the most rapid of all the systems, since gravitational radiation is strongest when masses are large and periods are short.

2 OBSERVATIONS

2.1 WHT/ULTRACAM

We observed ES Ceti with the high-speed CCD camera ULTRACAM (Dhillon et al. 2007) mounted on the 4.2-m William Herschel Telescope (WHT) in 2005 and 2010. ULTRACAM is a triple-beam camera, and all observations were made using the Sloan Digital Sky Survey (SDSS) u' , g' and r' or i' filters. The CCDs were windowed in order to obtain exposure times of 2–4 s, depending on conditions. The dead time between exposures for ULTRACAM is ~ 25 ms. In 2005, we observed ES Ceti five times over the period 2005 August 27–September 01. Conditions were good, with seeing < 1 arcsec and good transparency. We observed ES Ceti once more on the night of 2010 January 07. These observations were affected by poorer seeing and some cloud.

All of these data were reduced with aperture photometry using the ULTRACAM pipeline software. We follow the same steps for reduction and flux calibration as detailed in our previous ULTRACAM publications (e.g. Copperwheat et al. 2010, 2011).

2.2 WHT/ACAM

We made a further observation of ES Ceti in excellent conditions on the night of 2010 August 22 with the WHT using the permanently

mounted imaging auxiliary-port camera (ACAM) (Benn, Dee & Agócs 2008). We used a 5-s exposure time and windowed the chip to reduce the readout time between exposures to ~ 0.8 s. These data were reduced in the same way as the ULTRACAM data.

2.3 SAAO and CBA observations

We supplemented our WHT observations with additional data collected with smaller telescopes over a longer time period. We observed ES Ceti with the University of Cape Town CCD photometer (O'Donoghue 1995), mounted on the 1.9-m telescope at the South African Astronomical Observatory (SAAO). This instrument was used in frame transfer mode and the observations were made in white light in order to maximize the count rate. Typical exposure times vary from 10 to 20 s. These data were reduced using the *DOPHOT* program (Schechter, Mateo & Saha 1993; O'Donoghue 1995). We discarded any data in which conditions, the exposure time or the length of the observation means that the photometric period is not readily apparent. This left us with 38 nights of observation obtained between 2001 October 18 and 2009 October 9. The length of each observation varied, but was typically between five and 10 orbital cycles.

We obtained additional nights of observation with the Center for Backyard Astrophysics (CBA) telescope network, a global network of small telescopes dedicated to photometry of CVs.¹ Typical exposure times for these observations were ~ 20 s. As with the SAAO data, we discarded any observations in which the photometric period is not obvious. This leaves us with 21 observations obtained between 2002 January 18 and 2010 January 1.

3 ULTRACAM LIGHT CURVES

We measured the flux from ES Ceti in 2005 using our ULTRACAM data and find the mean magnitudes to be 15.94, 16.28, 16.63 and 17.23 in u' , g' , r' and i' , respectively. We found the object to be slightly fainter in 2010, with mean magnitudes of 16.19, 16.35 and 16.73 in u' , g' and r' . The amplitude of the light curve varies between bands but is 0.11–0.18 on average.

Using the ephemeris given in Section 4, we phase folded our ULTRACAM and ACAM data and plot the results in Fig. 1. We do not combine data from multiple nights, since Espaillat et al. (2005) showed evidence for some variation in the shape of the light curve on different nights. We also observe these changes in our data: while each light curve is roughly sinusoidal with the minimum light consistently at the phase of zero, on August 2005 28 and 29 we see a secondary minimum at a phase of ~ 0.35 , which is not present in the other three light curves obtained in 2005. The two 2010 light curves may be intermediate between the two states observed in 2005. The time-scale over which the light-curve shape can change is very short: an examination of the unfolded light curves shows significant changes over the course of a few orbital cycles. The cause of this variation is unclear, but it is most likely associated with the accretion disc.

4 ORBITAL TIMINGS

In order to measure the photometric period in ES Ceti, we choose to fit a simple function to each night of data. We found that the

¹ More details concerning the CBA can be found at <http://cba.phys.columbia.edu>.

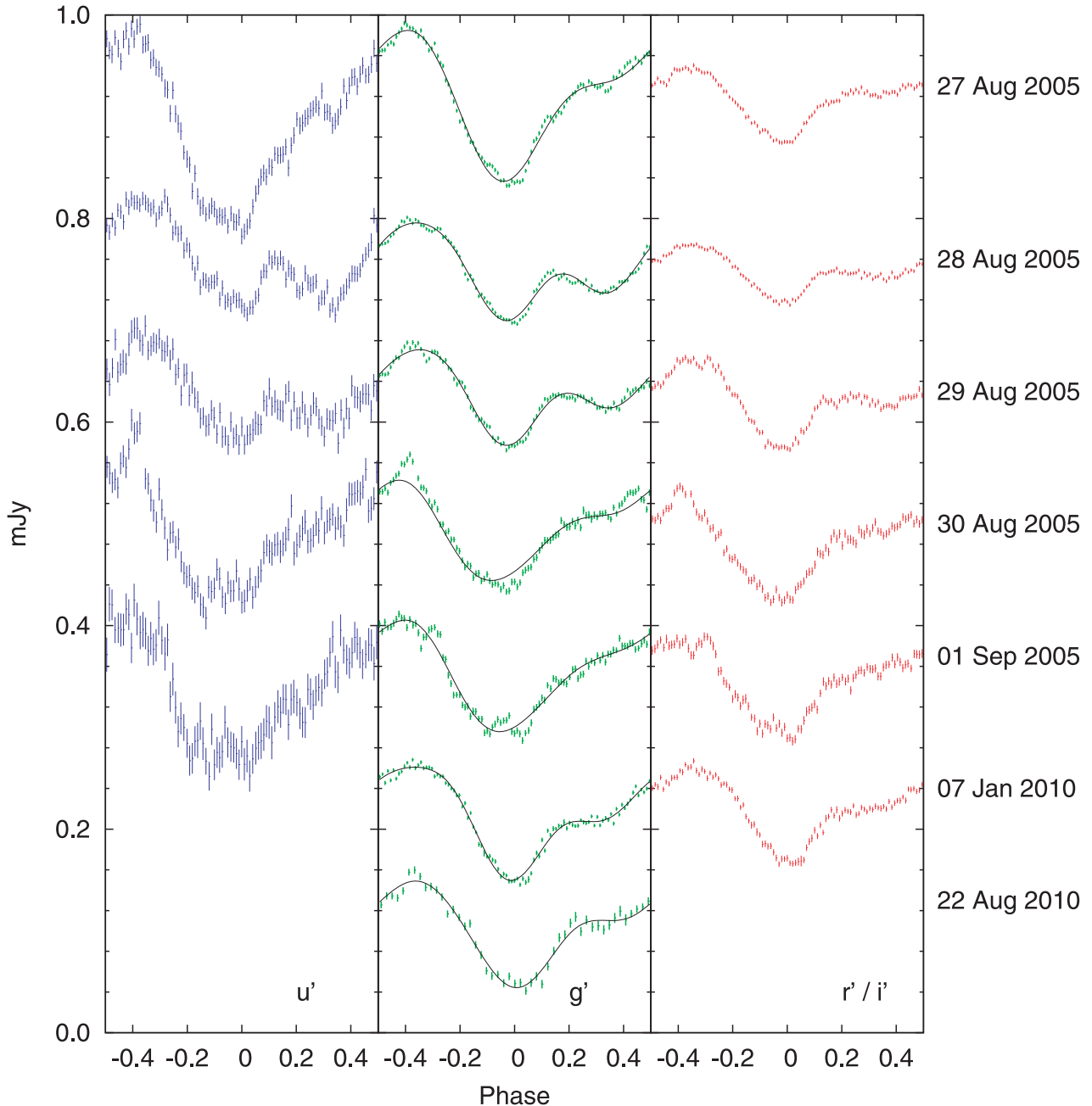


Figure 1. Phase-folded ULTRACAM and ACAM light curves. Due to the significant variations in the light curves from night to night, we phase fold the data on a night by night basis. The u' -band light curves are plotted in the left-hand panel, the g' -band light curves in the middle, and the right-hand panel contains either the i' -band (nights 1 and 2) or r' -band (nights 3–6) light curves. We omit the u' -band light curve for night 6, which was particularly affected by poor weather conditions. A flux offset is applied to each light curve for clarity. For the g' -band data we over plot the fits as detailed in Section 4, consisting of three sinusoids at the fundamental orbital frequency and its first and second harmonics.

variation in ES Cet is fitted well on any given night by the sum of three sinusoids of the form $f(t) = a_n \cos(2\pi n(t - t_0 - t_n)/P)$, where n is 1, 2 or 3, hence these sinusoids correspond to the fundamental orbital frequency and the first and second harmonics. P is the orbital period and t_0 is the time of minimum light. We fitted this function to each night of ULTRACAM g' -band data (in which the signal-to-noise ratio is highest). These fits are over-plotted on the g' -band data in Fig. 1. We first set t_0 to 0 and P to 1 and fit the function to the phase-folded light curve in order to determine a_n and t_n . We then determined t_0 from the unfolded light curve by fixing a_n and

t_n and fitting the function to these data. The process of fitting the data is complicated by the variable shape of the light curve, which we discussed in Section 3. This particularly complicates the task of fitting the CBA/SAAO observations, which have a much lower cadence than our WHT observations. It is therefore difficult to fit most of the observations with the same degree of precision with which we fit the WHT observations.

Furthermore, we find that our determination of the light-curve minimum t_0 is perturbed by the changing light-curve shape. This is apparent in the 2005 ULTRACAM timings. These were collected

over the course of a few successive nights, and so when the linear ephemeris is subtracted they should have similar O–C values. We find the O–C values to form two groups with a significant offset of around 20 s (with a formal error on the individual timings of ~ 1 s). These two groups correspond to the two distinct light-curve shapes observed in Fig. 1. In an attempt to characterize this effect with the aim of subtracting it from our light curves, we fitted each night separately and examined the variation in the model parameters with the O–C excess from a linear ephemeris. We found first of all that the model parameters can take a continuous range of values between the two extreme states we observed with ULTRACAM, and we observed a scatter of up to ~ 25 s in the timings. Some component of this scatter is doubtless due to flickering, the stochastic variation observed in all accreting systems; but a large component is due to the gross changes in the light curve. We observed a loose correlation between the O–C values and the amplitude and phase of the first harmonic. We attempted to improve our O–C residuals by adding an offset determined from these correlations, but since the correlation is fairly weak our timings were not improved to any significant degree. The limitation here is most likely the difficulty in fitting the majority of our observations with precision, due to the low time resolution and the gross variation of the light curve on time-scales of a few cycles. Since any improvement is very small, we chose not to apply any correction of this nature to our final determinations of the orbital timings.

For consistency, we obtain our final timings by applying the same model fit to each night, allowing t_0 to vary but fixing a_n and t_n . In practice, we found it does not matter which night of ULTRACAM data we use for these a_n and t_n values, but we choose night 6 since the light-curve shape in this case is intermediate between the two extremes. We did try phase folding and fitting each night separately, and then using the fit for each night to determine the time of minimum light for that individual night, but this did not improve the timings to any significant degree and in some cases made things worse due to the uncertainty of the fits. We obtain 65 timings in total, which we list in Table 1. Our final set of timings is in good agreement (rms ~ 6 s) with the measurements of Espaillat et al. (2005) for the cases where we share data. We convert all timings to the barycentric dynamical time-scale, correcting for light travel times.

Finally, using these timings, we calculate an ephemeris of

$$\text{BMJD(TDB)} = 52200.980\,575(6) + 0.007\,178\,375\,98(3)E$$

for the minimum-light point of the orbital cycle, using a linear least-squares fit. The data points in Fig. 2 show the residuals after this linear fit is subtracted and demonstrates that there is no significant departure from linearity over the baseline of our observations.

5 DISCUSSION

In this section, we examine the period change in ES Ceti over the baseline of our observations. In Section 5.1, we discuss the period changes and subsequent departure from a linear ephemeris in AM CVn systems as a result of gravitational radiation. We then compare these models to our ES Ceti timings in Section 5.2.

5.1 Period changes in accreting binaries

The fractional period change in an accreting binary system can be shown to be

$$\frac{\dot{P}}{P} = 3 \left(\frac{\dot{J}}{J} - (1 - q) \frac{\dot{M}_2}{M_2} \right), \quad (1)$$

Table 1. Our minimum-light timings for ES Ceti, using the sine function fit described in Section 4. We determine the uncertainties by fitting a large number of data sets, resampled from the original data using the bootstrap method (Efron 1979; Efron & Tibshirani 1993). For each timing, we indicate if it was obtained by SAAO (S), CBA (C), ULTRACAM (U) or ACAM (A).

	Cycle	BMJD		Cycle	BMJD
S	0	52200.98063(3)	C	57 688	52615.08678(6)
S	134	52201.94270(3)	C	60 619	52636.12651(3)
S	274	52202.94762(3)	S	60 994	52638.81849(10)
S	433	52204.08908(3)	S	83 192	52798.16412(4)
C	12 698	52292.13155(4)	S	93 497	52872.13709(5)
C	12 838	52293.13636(3)	S	93 779	52874.16180(6)
C	16 596	52320.11289(4)	S	97 951	52904.10985(5)
S	16 831	52321.79975(7)	S	99 892	52918.04294(5)
S	16 968	52322.78333(5)	S	134 317	53165.15846(4)
S	17107	52323.78128(5)	S	134 875	53169.16426(7)
S	43614	52514.05836(2)	S	146 279	53251.02627(6)
S	43745	52514.99882(4)	S	146 847	53255.10348(3)
S	44162	52517.99198(3)	S	167 703	53404.81578(7)
C	47844	52544.42274(3)	S	167 841	53405.80629(6)
C	47982	52545.41327(2)	S	167 981	53406.81140(8)
C	48121	52546.41115(2)	U	196 318	53610.22484(1)
C	48392	52548.35663(4)	U	196 454	53611.20136(1)
C	48675	52550.38796(2)	U	196 595	53612.21349(1)
S	48763	52551.01975(3)	U	197 006	53615.16357(2)
S	49035	52552.97227(4)	S	245 612	53964.07579(4)
S	49051	52553.08725(4)	S	245 762	53965.15266(7)
C	49096	52553.41030(3)	C	259 428	54063.25214(5)
S	49158	52553.85520(5)	C	265 117	54104.09019(8)
S	49181	52554.02031(3)	C	315 130	54463.10209(8)
C	49 235	52554.40809(4)	C	317 361	54479.11720(6)
S	49 302	52554.88571(38)	C	319 869	54497.12051(5)
S	49 441	52555.88667(4)	C	359 186	54779.35267(4)
C	49 509	52556.37485(2)	S	405 672	55113.04683(4)
S	52 360	52576.84022(5)	C	417 121	55195.23200(8)
S	52 535	52578.09646(8)	C	417 387	55197.14168(5)
S	54 316	52590.88107(6)	U	418 324	55203.86763(2)
S	56 127	52603.88493(28)	A	449 996	55431.22123(2)
S	56 682	52607.86516(5)			

(Marsh & Nelemans 2005) assuming conservative mass transfer, and where $q = M_2/M_1$, M_1 and M_2 are the masses of the accretor and donor, respectively, and \dot{M}_2 is the mass transfer rate. The corresponding quadratic time shift in the times of light-curve minima is given by

$$\Delta T = \frac{1}{2} \left(\frac{\dot{P}}{P} \right) t_B^2, \quad (2)$$

where t_B is the baseline of our observations. Assuming that the spin of the accretor is strongly coupled to the orbit (see Marsh, Nelemans & Steeghs 2004), the \dot{J} term in equation (1) is simply due to gravitational radiation, where

$$\frac{\dot{J}_{\text{GR}}}{J_{\text{orb}}} = -\frac{32}{5} \frac{G^3}{c^5} \frac{M_1 M_2 M}{a^4}, \quad (3)$$

(Landau & Lifshitz 1975), where a is the orbital separation. Since $\dot{J}/J < 0$ in the absence of mass transfer, we would expect a decreasing period as the two components spiral in. In an accreting system, the \dot{M}_2 term in equation (1) can compensate for \dot{J} (since $\dot{M}_2 < 0$) and for the expected mass transfer rates in AM CVn stars it is larger, and so we expect a lengthening period in these systems once it has settled into its long-term, stable state. It can be shown

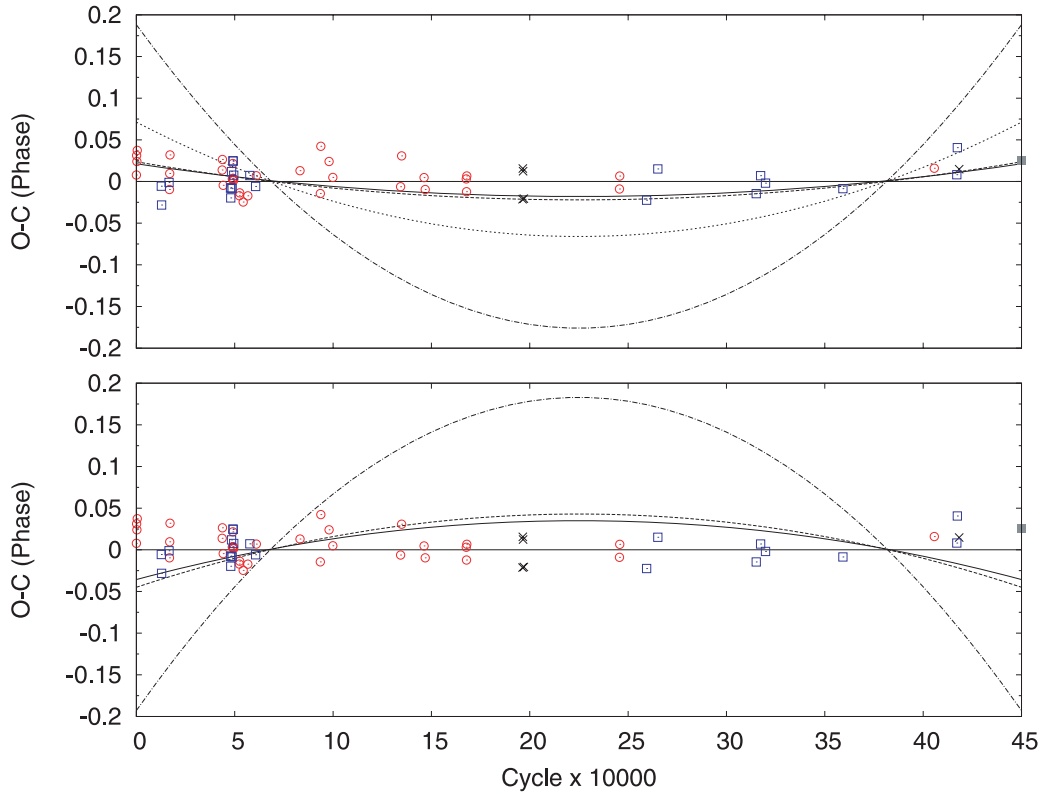


Figure 2. Top panel: minimum-light timings for our complete data set. We plot the period excess (O–C) in terms of phase against the orbital cycle. ULTRACAM observations are denoted by the black crosses, SAAO observations by the unfilled red circles, CBA observations by the unfilled blue squares and the ACAM observation by the filled grey square. The four curved lines indicate the expected period change when we include mass transfer at the secular rate, for different combinations of accretor and donor mass. The four combinations are the following. (i) Solid line, $M_1 = 0.44 M_\odot$, $M_2 = 0.062 M_\odot$, $\zeta_2 = -0.28$. This is the minimum period change, assuming accretion via a disc and a fully degenerate donor. (ii) Dashed line, $M_1 = 0.60 M_\odot$, $M_2 = 0.062 M_\odot$, $\zeta_2 = -0.28$. This is a variation on the minimum case in which we assume a more likely accretor mass. (iii) Dot–dashed line, $M_1 = 0.69 M_\odot$, $M_2 = 0.26 M_\odot$, $\zeta_2 = -0.28$. Here we assume a partially degenerate donor using the M–R relation for the He–star formation channel (Nelemans et al. 2001) and the corresponding minimum accretor mass. We use the same value of ζ_2 as for the fully degenerate models. This is unlikely to be correct, and so in (iv) (dotted line), we set $\zeta_2 = 0$, keeping all other parameters the same. The true value of ζ_2 will be between these two extremes, but is likely to be closest to 0. Bottom panel: as with the top panel, except here we assume the secondary star is detached from its Roche lobe, and so the binary evolution proceeds due to gravitational radiation in the absence of mass transfer. In this detached case, models (iii) and (iv) give the same prediction, since they are only distinguished from each other by the response of the donor to mass-loss.

that

$$\frac{\dot{M}_2}{M_2} = \frac{\dot{J}/J}{1 + (\zeta_2 - \zeta_{RL})/2 - q} \quad (4)$$

(Marsh et al. 2004), where

$$\zeta_2 = \frac{d \log R_2}{d \log M_2}, \quad (5)$$

and

$$\zeta_{RL} = \frac{d \log(R_{RL}/a)}{d \log M_2} \quad (6)$$

describe the response of the donor and the Roche lobe to mass transfer. ζ_{RL} is taken to be $1/3$ using the small q approximation of Paczyński (1971). Since the response of a degenerate star is to expand on mass-loss, ζ_2 is < 0 . A value of $\zeta_2 = -0.28$ is appropriate for a fully degenerate donor, but as the degree of degeneracy of the donor is decreased, ζ_2 approaches 0 (Deloye, Bildsten & Nelemans 2005).

5.2 The period evolution in ES Cet

In this section, we compare our measurements of the orbital timings with the predicted time shift over our baseline. We see in

Section 5.1 that the predicted time shift depends on the masses of the donor star and the accretor. We begin in Section 5.2.1 by selecting various appropriate values for these unknown parameters. We then compare our timings with the expectations for these parameters in Sections 5.2.2 and 5.2.3. We consider first the case in which there is mass transfer between the two components. We also consider the detached case, in which there is no mass transfer and the period decreases at the rate given by equation (1) with $\dot{M}_2 = 0$. However, given that the spectral observations imply accretion, we would expect the first case to be a better fit to our data.

5.2.1 The component masses

There are three formation paths proposed for AM CVn stars. All three paths are consistent with a donor that is partially degenerate to some degree, and measurements of the component masses in other AM CVn systems have confirmed the donors to be partially degenerate (Roelofs et al. 2006, 2007a; Copperwheat et al. 2011). The ‘white dwarf channel’ (Nelemans et al. 2001) suggests detached close double white dwarfs which are brought into contact as a result of angular momentum loss due to gravitational wave radiation (GWR). Nelemans et al. (2001) used a fully degenerate, zero-temperature donor in their formulation, but Deloye et al. (2005)

argued that the donors could be semidegenerate depending on the contact time of the binary. The second scenario is the ‘evolved CV channel’ (Podsiadlowski, Han & Rappaport 2003) which suggests the progenitors of AM CVn stars are CVs with evolved secondaries. The donor in this channel is initially non-degenerate and hydrogen rich, but becomes degenerate and helium rich (but still with a few per cent hydrogen) during its evolution before Roche lobe overflow. The third scenario is the ‘helium star channel’ (Iben & Tutukov 1991), in which the donor had been a helium core burning star before coming into contact with its Roche lobe. For the white dwarf and evolved CV channels, the donor mass is somewhat arbitrary, since it depends on factors such as the specific entropy of the donor at time of contact (Deloye et al. 2005). We therefore chose to examine two cases: first in which the donor is fully degenerate and secondly, in which it has a mass consistent with a helium star progenitor. The helium star channel implies a very massive donor star, and the expected mass for the other two channels will lie between these two extremes.

If we assume a fully degenerate donor, we find M_2 to be $0.062 M_\odot$ (Deloye et al. 2005). This is the lowest possible mass for the donor in this system. We chose to combine this with the lowest likely accretor mass M_1 , since the case in which both M_1 and M_2 are at their lowest values produces the minimum period change in both the accreting and non-accreting formulations. For this, we assumed the system is accreting via a disc, rather than through the direct impact of the accretion stream on to the white dwarf primary. We believe accretion via a disc is a reasonable assumption, since the spectroscopic data do feature the double-peaked lines which are characteristic of an accretion disc although the direct-impact scenario cannot be ruled out entirely, since even in this case the primary Roche lobe might be filled with diffuse, hot gas which could produce a ‘disc-like’ signature in the spectra (Roelofs et al. 2010). The presence of an accretion disc implies a minimum mass for the accretor (for a given donor mass) simply via geometric arguments, since the accretion stream follows a ballistic trajectory. For a donor mass of $0.062 M_\odot$, the minimum possible mass for the accretor is $0.44 M_\odot$. This accretor mass is quite low, so we also considered a higher accretor mass of $\sim 0.6 M_\odot$, which is more typical of field white dwarfs. Since the donor is fully degenerate, we set $\zeta_2 = -0.28$.

For the partially degenerate case, we use the Nelemans et al. (2001) fit to the He-star mass–radius (M – R) track of Tutukov & Fedorova (1989) to determine the donor mass. Fig. 1 of Deloye et al. (2005) shows that the predicted donor mass for this scenario is $\sim 0.26 M_\odot$. We again assume the accretor mass to be at the minimum for accretion via a disc, which for this donor mass is $0.69 M_\odot$. The value of ζ_2 in this case is not clear but will lie somewhere between 0 and the fully degenerate value of -0.28 . Given that the donor star we consider here is considerably less degenerate than the $M_2 = 0.062 M_\odot$ case, we would expect ζ_2 to be closer to 0, but we consider both of these two extremes.

5.2.2 Period evolution with mass transfer

We plot in Fig. 2 the deviation from a linear ephemeris for our orbital timings in terms of phase, using the linear ephemeris given in Section 4. If we examine the data points first of all, we see a large scatter (as discussed in Section 4) is apparent in these timings (in particular, note the separation between the two groups of 2005 ULTRACAM timings, at $\sim 200\,000$ cycles). However, aside from this random variation, there is no obvious departure from a linear ephemeris over the baseline of our observations. There might be

a very small increase in period over our baseline (manifested by a slightly positive O–C value at either extreme of the plot and a slightly negative value in the middle); however any such trend does not appear to be very significant when compared to the noise.

The curved lines in the top panel of Fig. 2 show the predicted departure from a linear ephemeris with $M_1 = 0.44 M_\odot$ and $M_2 = 0.062 M_\odot$ (solid line), $M_1 = 0.6 M_\odot$ and $M_2 = 0.062 M_\odot$ (dashed line), and $M_1 = 0.69 M_\odot$ and $M_2 = 0.26 M_\odot$ (the dot–dashed and dotted lines, for a ζ_2 of -0.28 and 0, respectively). All four predict an increasing period as a result of the mass transfer. These lines have been vertically offset to optimize the fit to the data. We see that in the cases where we assume a fully degenerate donor, the predicted time shift is very small, and the amplitude is less than the uncertainty in our data points. A fully degenerate donor is therefore consistent with our timings. Increasing the mass of the accretor has little effect on these amplitudes. Conversely, the predicted time shift when a donor mass of $M_2 = 0.26 M_\odot$ is used is much larger. When we set ζ_2 to -0.28 it is very large and clearly precluded by our measurements. As ζ_2 is increased, the response of the donor to mass-loss is decreased, and so the expected time shift over our baseline is also decreased. The exact value of ζ_2 for this semidegenerate donor is likely close to (but not greater than) 0. The dotted line in Fig. 2 shows that even when we set $\zeta_2 = 0$, the predicted deviation from linearity is not consistent with our timings if we assume a massive donor.

We have shown that the He-star formation channel produces a donor that is too massive to be consistent with our timings. If we examine the evolutionary tracks given in Podsiadlowski et al. (2003) for the evolved CV channel, we find that, while the donor mass is dependent on initial conditions, a reasonable assumption for the donor mass is 0.11 – $0.12 M_\odot$, which also predicts a deviation from linearity which is inconsistent with our timings. We conclude therefore that the double white dwarf channel is the most likely formation path for the low donor mass we infer.

An alternative explanation is that ES Ceti is in the initial, turn-on phase before the long AM CVn phase of lengthening period, and so the accretion rate in ES Ceti is currently below the stable rate which would be expected if it were in that phase. The decreasing periods of HM Cnc and V407 Vul have been explained by invoking an accretion model in which the donor has a thin hydrogen envelope, and it is the accretion of this envelope which leads to the shortening period (D’Antona et al. 2006). At some point, this envelope will be depleted and the transfer of helium will begin, leading to a lengthening period along the ‘traditional’ evolutionary track. As the binary transitions from one state to the other, the fractional period change must drop significantly. Since we find ES Ceti to be consistent with a \dot{P} of 0, it could now exist in this intermediate regime, linking HM Cnc and V407 Vul with the longer period AM CVn stars.

Finally, we note that one assumption we have made is that all of the angular momentum contained in the mass gained by the accretor from the donor is fed back into the orbit. Alternatively, some fraction of the disc accretion may act to spin up the accretor. However, we find that this only increases the expected \dot{P} and so does not improve the fit of any of our models to the observed timings. If we consider the extreme case, in which none of the angular momentum is fed back to the orbit, equation (4) is modified to

$$\frac{\dot{M}_2}{M_2} = \frac{\dot{J}/J}{1 + (\zeta_2 - \zeta_{RL})/2 - q - \sqrt{(1+q)R_1/a}} \quad (7)$$

(Marsh et al. 2004), where R_1 is the accretor radius and a is the binary separation. This extreme case predicts a deviation from linearity of

0.23 or 0.32 in phase over our baseline, assuming a fully degenerate donor and an accretor mass of 0.60 or 0.45 M_{\odot} . This is clearly inconsistent with our timings, suggesting that a substantial fraction of the angular momentum is indeed fed back into the orbit.

5.2.3 Period evolution with no mass transfer

We consider also the scenario in which the donor star is detached from its Roche lobe. In this case, the period will decrease as the components spiral in as angular momentum is lost due to gravitational radiation. The three curved tracks in the bottom panel of Fig. 2 show the predicted departure from a linear ephemeris for the detached case, for the same combinations of M_1 and M_2 used in the top panel. All three lines are a poorer fit to our timings compared to the corresponding semidetached scenarios, as expected given the evidence of accretion.

6 CONCLUSIONS

We have obtained high time resolution light curves of the AM CVn star ES Cet with WHT+ULTRACAM and other smaller telescopes around the world. We observed the previously reported cyclical variability which has been confirmed to be orbital in origin. Our observations cover a baseline of 9 yr and we fit the light curves to obtain precise orbital timings over that period. We find that there is no evidence for a deviation from a linear ephemeris over this time period, although scatter in the timings is high due to flickering and large cycle-to-cycle variations in the light-curve shape. There may be an underlying trend which is masked by this scatter. However, many predictions do suggest a lengthening orbital period which should be clearly detectable over this noise. Our findings suggest a low mass for the donor star, close or equal to the zero-temperature mass of 0.062 M_{\odot} . This would make the double white dwarf formation channel the most likely scenario for this system. Alternatively, the accretion rate in this system may be significantly below the long-term, secular rate for an accreting AM CVn star. ES Cet is the shortest period AM CVn star, and the only ultracompact binaries with shorter periods are HM Cnc and V407 Vul, both of which have been shown to have a decreasing period. ES Cet may be in an intermediate phase between these systems and the longer period AM CVn stars.

ACKNOWLEDGMENTS

CMC and TRM are supported under grant ST/F002599/1 from the Science and Technology Facilities Council (STFC). ULTRACAM, SPL and VSD are supported by STFC grants PP/D002370/1 and PP/E001777/1. DS acknowledges the support of an STFC Advanced Fellowship. PAW and BW are supported by the National Research Foundation and the University of Cape Town. The results presented in this paper are based on observations made with the WHT operated on the island of La Palma by the Isaac Newton Group in the Spanish Observatorio del Roque de los Muchachos of the Instituciones de Astrofísica de Canarias. This research has made use of NASA's Astrophysics Data System Bibliographic Services and the SIMBAD database, operated at CDS, Strasbourg, France. We thank Lars Bildsten for helpful discussions.

REFERENCES

- Benn C., Dee K., Agócs T., 2008, in Mclean I. S., Casali M. M., eds, Proc. SPIE Conf. Ser. Vol. 7014, ACAM: a new imager/spectrograph for the William Herschel Telescope. SPIE, Bellingham, p. 229
- Bildsten L., Shen K. J., Weinberg N. N., Nelemans G., 2007, ApJ, 662, L95
- Copperwheat C. M., Marsh T. R., Dhillion V. S., Littlefair S. P., Hickman R., Gänsicke B. T., Southworth J., 2010, MNRAS, 402, 1824
- Copperwheat C. M. et al., 2011, MNRAS, 410, 1113
- D'Antona F., Ventura P., Burderi L., Teodorescu A., 2006, ApJ, 653, 1429
- Deloye C. J., Taam R. E., 2006, ApJ, 649, L99
- Deloye C. J., Bildsten L., Nelemans G., 2005, ApJ, 624, 934
- Dhillion V. S. et al., 2007, MNRAS, 378, 825
- Di Stefano R., 2010, ApJ, 719, 474
- Efron B., 1979, Ann. Statistics, 7, 1
- Efron B., Tibshirani R. J., 1993, An Introduction to the Bootstrap. Chapman & Hall, New York
- Espallat C., Patterson J., Warner B., Woudt P., 2005, PASP, 117, 189
- Farmer A., Roelofs G., 2010, (arXiv:1006.4112)
- Gilfanov M., Bogdán Á., 2010, Nat, 463, 924
- Haberl F., Motch C., 1995, A&A, 297, L37
- Hakala P., Ramsay G., Wu K., Hjalmarsdotter L., Järvinen S., Järvinen A., Cropper M., 2003, MNRAS, 343, L10
- Hakala P., Ramsay G., Byckling K., 2004, MNRAS, 353, 453
- Iben I. J., Tutukov A. V., 1991, ApJ, 370, 615
- Kasliwal M. M. et al., 2010, ApJ, 723, 98
- Kotak R., 2008, in Evans A., Bode M. F., O'Brien T. J., Darnley M. J., eds, ASP Conf. Ser. Vol. 401, Progenitors of Type Ia Supernovae. Astron. Soc. Pac., San Francisco, p. 150
- Landau L. D., Lifshitz E. M., 1975, The Classical Theory of Fields. Pergamon Press, Oxford
- Marsh T. R., 1999, MNRAS, 304, 443
- Marsh T. R., Nelemans G., 2005, MNRAS, 363, 581
- Marsh T. R., Steeghs D., 2002, MNRAS, 331, L7
- Marsh T. R., Nelemans G., Steeghs D., 2004, MNRAS, 350, 113
- Morales-Rueda L., Marsh T. R., Steeghs D., Unda-Sanzana E., Wood J. H., North R. C., 2003, A&A, 405, 249
- Nelemans G., Portegies Zwart S. F., Verbunt F., Yungelson L. R., 2001, A&A, 368, 939
- Nelemans G., Yungelson L. R., Portegies Zwart S. F., 2004, MNRAS, 349, 181
- Nelemans G., Yungelson L. R., van der Sluys M. V., Tout C. A., 2010, MNRAS, 401, 1347
- O'Donoghue D., 1995, Baltic Astron., 4, 519
- Paczyński B., 1971, ARA&A, 9, 183
- Podsiadlowski P., Han Z., Rappaport S., 2003, MNRAS, 340, 1214
- Ramsay G., Hakala P., Marsh T., Nelemans G., Steeghs D., Cropper M., 2005, A&A, 440, 675
- Roelofs G. H. A., Groot P. J., Nelemans G., Marsh T. R., Steeghs D., 2006, MNRAS, 371, 1231
- Roelofs G. H. A., Groot P. J., Benedict G. F., McArthur B. E., Steeghs D., Morales-Rueda L., Marsh T. R., Nelemans G., 2007a, in Napiwotzki R., Burleigh M. R., eds, ASP Conf. Ser. Vol. 372, The Nature of the Donor Stars in Ultra-Compact AM CVn Binaries. Astron. Soc. Pac., San Francisco, p. 437
- Roelofs G. H. A., Nelemans G., Groot P. J., 2007b, MNRAS, 382, 685
- Roelofs G. H. A., Rau A., Marsh T. R., Steeghs D., Groot P. J., Nelemans G., 2010, ApJ, 711, L138
- Schechter P. L., Mateo M., Saha A., 1993, PASP, 105, 1342
- Solheim J., 2010, PASP, 122, 1133
- Stroeer A., Vecchio A., 2006, Classical Quantum Gravity, 23, 809
- Strohmayer T. E., 2005, ApJ, 627, 920
- Tutukov A. V., Fedorova A. V., 1989, Soviet Astron., 33, 606
- Warner B., Woudt P. A., 2002, PASP, 114, 129
- Willems B., Kalogera V., 2005, ArXiv e-prints (astro-ph/0508218)
- Wu K., Cropper M., Ramsay G., Sekiguchi K., 2002, MNRAS, 331, 221

This paper has been typeset from a $\text{\TeX}/\text{\LaTeX}$ file prepared by the author.